Cell. Mol. Biol. (ISSN: 1165-158X)

Journal Homepage: www.cellmolbiol.org

Cellular and Molecular Biology

Original Article

Computational identification of promising therapeutics via BACE1 Targeting: Implications for Alzheimer's disease

Hussam Aly Sayed Murad[1], Mamdoh S. Moawadh[2], Abdulrahman Alzahrani[3], Ahmad Salah Alkathiri[4], Abdulrahman Almutairi[5], Madawi Ibrahim Alhassoun[5], Rashed Ahmed Alniwaider[6], Alaa Hamed Habib[7], Ziaullah M Sain[8], Misbahuddin M Rafeeq[1*]

[1] Department of Pharmacology, Faculty of Medicine, Rabigh, King Abdulaziz University, Jeddah, Saudi Arabia
[2] Medical Laboratory Technology, Faculty of Applied Medical Sciences, University of Tabuk Saudi Arabia
[3] Department of Applied Medical Sciences, Applied College, Al-Baha University, Al-Baha City, Kingdom of Saudi
[4] Department of Health Promotion and Education, Faculty of Public Health & Health Informatics, Umm Al-Qura University, Makkah, Kingdom of Saudi Arabia
[5] Department of Pathology and Laboratory Medicine, Ministry of National Guard Hospital and Health Affairs (MNGHA), P.O.box 22490, Kingdom of Saudi Arabia
[6] Toxicology Laboratory Department of Pathology and Laboratory Medicine, Ministry of National Guard Hospital and Health Affairs (MNGHA), P.O. box 22490, Kingdom of Saudi Arabia
[7] Department of Physiology, Faculty of Medicine, King Abdulaziz University, Jeddah, Saudi Arabia
[8] Department of Microbiology, Faculty of Medicine, Rabigh. King Abdulaziz University. Jeddah, 21589, KSA

Article Info

Article history:

Received: December 21, 2023
Accepted: April 03, 2024
Published: August 31, 2024

Use your device to scan and read the article online

Abstract

Alzheimer's disease (AD) is a significant global healthcare challenge, particularly in the elderly population. This neurodegenerative disorder is characterized by impaired memory and progressive decline in cognitive function. BACE1, a transmembrane protein found in neurons, oligodendrocytes, and astrocytes, exhibits varying levels across different neural subtypes. Abnormal BACE1 activity in the brains of individuals with AD leads to the formation of beta-amyloid proteins. The complex interplay between myelin sheath formation, BACE1 activity, and beta-amyloid accumulation suggests a critical role in understanding the pathological mechanisms of AD. The primary objective of this study was to identify molecular inhibitors that target Aβ. Structure-based virtual screening (SBVS) was employed using the MCULE database, which houses over 2 million chemical compounds. A total of 59 molecules were selected after the toxicity profiling. Subsequently, five compounds conforming to the Egan-Egg permeation predictive model of the ADME rules were selected and subjected to molecular docking using AutoDock Vina on the Mcule drug discovery platform. The top two ligands and the positive control, 5HA, were subjected to molecular dynamics simulation for five nanoseconds. Toxicity profiling, physiochemical properties, lipophilicity, solubility, pharmacokinetics, druglikeness, medicinal chemistry attributes, average potential energy, RMSD, RMSF, and Rg analyses were conducted to identify the ligand MCULE-9199128437-0-2 as a promising inhibitor of BACE1.

Keywords: SBVS, MD simulation, Molecular docking, RMSD, RMSF, ADME , AutoDoc.

1. Introduction

Alzheimer's disease (AD), a complex neurodegenerative condition, primarily affects the elderly and is the leading cause of dementia, characterized by cognitive decline and memory loss in individuals aged 65 years and older. First identified by Dr. Alois Alzheimer in 1906, AD has become a significant public health challenge affecting millions of individuals and their families. Its prevalence is projected to increase from 5.8 million to 13.8 million by 2050, emphasizing the need for comprehensive understanding and effective interventions [1, 2]. The exact causes of AD remain unclear, and a combination of genetic and environmental factors is believed to contribute to its onset. Genetic factors such as the presence of the APOE ε4 allele and other risk factors, such as cardiovascular conditions, diabetes, and head injuries, have been associated with increased susceptibility to AD [3-10].

The accumulation of beta-amyloid plaques, synaptic degeneration, and neurofibrillary tangles in the brain characterizes the pathophysiology of AD. Beta-amyloid plaques are extracellular deposits of misfolded proteins that disrupt normal neuronal function. In contrast, neurofibrillary tangles consist of twisted tau proteins within neurons, causing structural damage and ultimately leading

* Corresponding author.
E-mail address: marafeeq@kau.edu.sa (M. M. Rafeeq).
Doi: http://dx.doi.org/10.14715/cmb/2024.70.8.8

to cell death. These changes primarily affect brain regions associated with memory and cognitive function. Contemporary research models focus on regulating the accumulation rate of beta-amyloid to impede the progression of Alzheimer's disease (AD). Advanced biomarkers play a crucial role in elucidating the underlying mechanisms of the disease, offering valuable insights into potential therapeutic strategies [11-17]. Amyloid precursor protein (APP), a type 1 transmembrane glycoprotein with various isoforms, is cleaved by BACE1, the primary beta-secretase in the brain, resulting in the formation of amyloid-beta peptides that contribute to AD progression [18-22].

BACE1 is a critical therapeutic target owing to its role in Aβ production. Inhibitors designed to target the catalytic site of BACE1 aim to slow disease progression. BACE2, a closely related enzyme, participates in physiological functions such as myelination and synaptic transmission; however, the primary focus in the context of AD remains on BACE1 [23-27]. Despite the lack of a cure for AD, various treatment strategies have been developed to alleviate symptoms and decelerate disease progression. These include medications, such as cholinesterase inhibitors and memantine, which target neurotransmitter imbalances to enhance cognitive function, and non-pharmacological interventions, such as cognitive stimulation and physical exercise, which constitute integral components of disease management [28, 29].

Ongoing research has explored novel avenues for understanding AD, including genetics, molecular pathways, and potential therapeutic targets. Early diagnosis remains challenging, and researchers are investigating biomarkers and advanced imaging techniques for accurate and early detection [30-32]. Developing effective preventive strategies and treatments requires technological advancements and increased awareness. Our research utilizes Pfizer's Lipinski rule and virtual screening techniques to identify potential ligands for BACE1 within the MCULE digital library. We then employed AutoDock Vina (ADV) for docking on MCULE's platform, followed by a thorough evaluation of toxicophores using the Egan-Egg model for human intestinal absorption (HIA) and blood-brain barrier (BBB) permeability. The topological polar surface area (TPSA) and water-octanol partition coefficient (WLOGP) were used as parameters in these tests. Compounds that passed these evaluations were subjected to comprehensive screening for various pharmacokinetic parameters, and the stability of the top ligands was evaluated through molecular dynamics (MD) simulations. Finally, a comparative analysis was conducted between the leading molecules and a reference drug to identify potential drug candidates for Alzheimer's disease (AD) via inhibition of BACE1.

2. Materials and Methods

2.1 Retrieval and optimization of BACE1 protein structure

The three-dimensional crystal structure of BACE1 (2B8L) was obtained from the RCSB PDB at a resolution of 1.70 Å (33, 34). To create a 3D input file suitable for docking tools, the protein part of the crystal structure was selected and unwanted heteroatoms, ions, and molecular entities were excluded. The CHARMm force field was then applied to optimize and minimize the structural configuration [35].

2.2 High-throughput Structure-Based Virtual Screening (SBVS)

An online drug discovery platform, Mcule, was utilized to explore smaller essential molecules by implementing a high-throughput Structure-Based Virtual Screening (SBVS) process. The Mcule library, which comprises hundreds of millions of ligands, is the source of these molecules. The SBVS process involves the establishment of fundamental property filters, such as adherence to the Lipinski rule of five (ROF: MW ≤ 500 Da; hydrogen bond donor HBD ≤ 5; hydrogen bond acceptor ≤ 10; LogP ≤ 5). Other criteria considered during the workflow were chiral center ≤ 3, rotatable bonds ≤ 4, ≤ 10 N and O atoms, ≥ 10 heavy atoms, and rings ≤ 3. The SBVS search parameters were set with a sample size of 100,000, a diversity selection of 1000, and a similarity threshold 0.85. The search was performed using the Open Babel linear fingerprint search algorithm [36–38].

2.3 Retrieval and optimization of BACE1 inhibitor structure

We obtained Beta-secretase Inhibitor IV, 5HA (CID: 5287532), from the PubChem database in standard data format. To facilitate further analysis, we converted the SDF-2D file of the inhibitor to a PDB-3D file format using the BIOVIA Discovery Studio. The optimization procedure for the inhibitor followed the same steps as those reported for BACE1 (25, 39, 40).

2.4 Computational docking utilizing AutoDock Vina for investigating molecular interactions

To analyze the molecular interactions between BACE1 and the compounds identified through Structure-Based Virtual Screening (SBVS), AutoDock Vina was used. The apoprotein segment of BACE1 was imported and designated as the reference target [41-44]. A grid size of 40 Å was allocated along the x-, y-, and z-axes. The grid box covering the protein-ligand binding site was defined with variable grid points along the x (29.026 Å), y (45.3075 Å), and z (15.4725 Å) axes. The minimum free energy of binding (ΔG) was selected as the discriminating parameter to identify the optimal binding affinities and positions for each ligand molecule docked within the active site of BACE1.

2.5 Exclusion of toxicophores

Following the molecular docking process, the top 100 molecules were subjected to toxicity profiling using the Mcule Toxicity Checker. This process involves the utilization of robust SMARTS (SMILES Arbitrary Target Specification) toxic matching rules to assess the presence of substructures, scaffolds, or moieties, commonly referred to as toxicophores, within chemical compounds.

2.6 Exploration of Absorption, Distribution, Metabolism, and Excretion (ADME) properties

Assessment of the absorptive, distributive, metabolic, and excretory properties of compounds is of utmost importance in understanding their effectiveness as drugs and their overall impact. This process involves classifying compounds based on their pharmacokinetic properties, and it is imperative to meet the criteria outlined by the ADME to achieve successful outcomes in laboratory experiments. The ADME characteristics of the compounds

were evaluated using the SwissADME web tool, considering various parameters such as drug-likeness, medicinal chemistry attributes, lipophilicity, and physiochemical properties [45-47].

2.7 Stability evaluation through Molecular Dynamics (MD) simulations

We performed computational simulations using the GROMACS 5.1.2 software to evaluate the stability of the two most promising protein-ligand docked complexes and the positive control. We utilized the GROMACS grep module to isolate the ligands from their complexes and the CHARMm General Force Field (CGenFF) server to assign topology and forcefield parameters. We created a topology for the PfBLM Helicase-ATP Binding Domain using pdb-2gmx segments in the GROMACS package. The structural coordinates of the top three hits were obtained using the CGenFF tool. Each complex was enclosed in a dodecahedron box filled with water molecules, ensuring a 10 Å margin around the complex. The charges in the complexes were neutralized and sodium and chloride ions were added to maintain a biological concentration of 0.15 M. We then performed an energy minimization process consisting of 250,000 steps, using a robust steepest descent algorithm. The temperature of the system was gradually increased from 0 to 300 K during a ten ns equilibration period at standard temperature and pressure (STP). After achieving equilibrium, a particle mesh was assigned using the Ewald scheme. We used various GROMACS modules to assess the stability of the hit molecules in terms of the root-mean-square deviation (RMSD), root-mean-square fluctuation (RMSF), and radius of gyration (Rg).

3. Results and Discussion

3.1 Rational selection of lead ligands through structure-Based Virtual Screening

In Structure-Based Virtual Screening (SBVS) facilitated by the Mcule online drug discovery platform, an extensive screening process was executed on a dataset of 2,208,042 ligand molecules. By employing rigorous criteria, including adherence to Lipinski's Rule of Five (RO5), drug-likeness parameters, and considerations of N and O atoms, as detailed in the methodology section [37], a subset of top-performing ligands emerged.

Following the initial screening, the top 100 ligands were further refined through toxicity profiling and assessment of the binding free energy. This rigorous selection process identified two exceptional ligands with ΔG values below -7.82 kcal/mol. These lead ligands, with ΔG values of -8.83 kcal/mol and -8.24 kcal/mol, respectively, were prioritized for subsequent simulation studies. This strategy is crucial for the development of novel drug candidates. The serial steps adopted are summarized in Figure 1.

3.2 Evaluation of toxicity for drug candidates

Evaluating a drug's pharmacokinetic properties is paramount in biological processes and may significantly impact subsequent stages, necessitating additional resources. In the initial stages of drug development, it is imperative to eliminate compounds that may be carcinogenic, mutagenic, or possess problematic scaffolds or toxicophores. Using the Mcule toxicity risk assessment, 59 compounds were deemed safe and potentially promising as drug candidates. The outcomes are summarized in Table 1.

3.3 Molecular docking (MD)

The binding affinities of all ligands and reference inhibitors (5HA) were evaluated by docking into the BACE1 binding pocket using the MCULE ADV tool. The calculated binding free energy (ΔG) for ligand hits ranged from -8.83 kcal/mol to -7.84 kcal/mol (Table 2).

A comparative analysis was conducted between docked complexes of the predicted ligands and BACE1, in contrast to the reference drug 5HA. The ΔG value of 5HA in its interaction with the BACE1 binding pocket was -7.82 kcal/mol, engaging with 16 residues through various binding interactions such as Van der Waals, conventional hydrogen bonds, carbon-hydrogen bond, Pi-Donor Hydrogen bond, Pi-Pi T-shaped, Amide-Pi Stacked, and Pi-Alkyl interactions (Figure 2A). Only five ligand hits from the toxicity checker demonstrated ΔG values lower than 5HA, as outlined in Table 2.

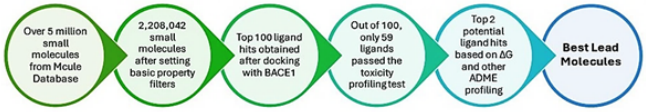

Fig. 1. SBVS schematic illustration for BACE1 lead molecule selection.

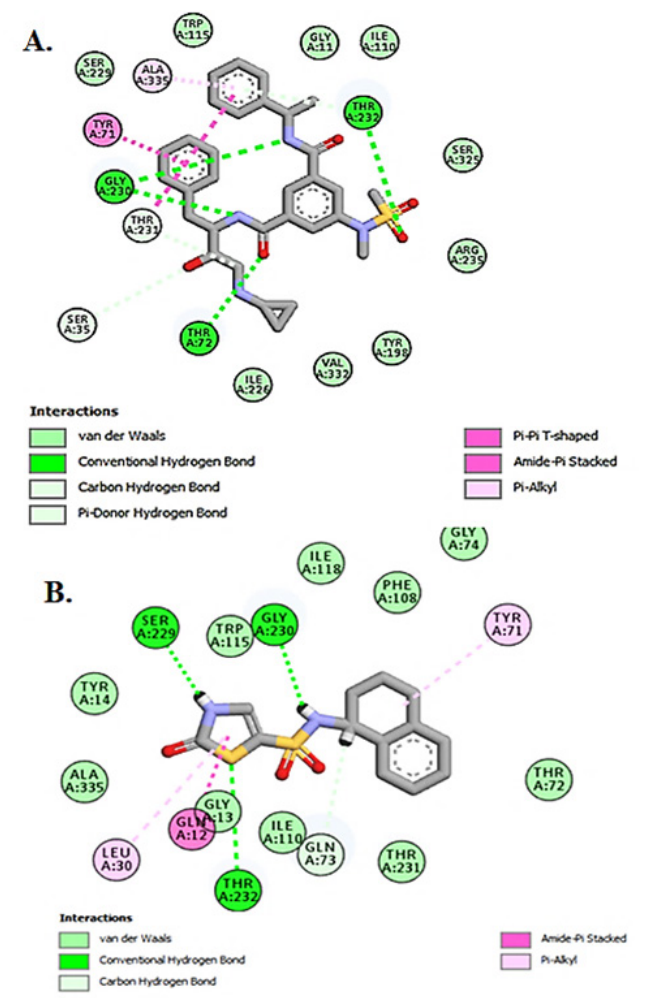

Fig. 2. (A) 2D representation of BACE1 and control molecule (5HA) interactions during docking, showcasing various forces **(B)** 2D illustration of BACE1 and MCULE-3872425295-0-7 interactions during docking, highlighting various forces.

Table 1. A comprehensive overview of the top 100 ligands, including mcule id and toxicity profiles.

S. No.	Ligand hits	Compliance with toxicity check
1.	MCULE-2491610851-0-1	Passed
2.	MCULE-9199128437-0-2	Passed
3.	MCULE-3872425295-0-7	Passed
4.	MCULE-6247779336-0-1	Failed
5.	MCULE-7785913432-0-10	Failed
6.	MCULE-8572723302-0-2	Passed
7.	MCULE-4983453402-0-1	Passed
8.	MCULE-3633236962-0-2	Failed
9.	MCULE-2831657328-0-2	Passed
10.	MCULE-9113665645-0-3	Failed
11.	MCULE-6573497537-0-2	Passed
12.	MCULE-4444541297-0-39	Failed
13.	MCULE-7106282644-0-1	Failed
14.	MCULE-7107671047-0-1	Failed
15.	MCULE-8150897678-0-4	Failed
16.	MCULE-6744001428-0-3	Failed
17.	MCULE-4676044378-0-2	Passed
18.	MCULE-2505328720-0-23	Passed
19.	MCULE-4963828787-0-2	Passed
20.	MCULE-3946806480-0-2	Passed
21.	MCULE-3952545513-0-1	Failed
22.	MCULE-8050325075-0-3	Passed
23.	MCULE-5979124564-0-3	Passed
24.	MCULE-2510260963-1-1	Failed
25.	MCULE-9884105036-0-1	Failed
26.	MCULE-3146454229-0-2	Passed
27.	MCULE-8110440589-0-1	Passed
28.	MCULE-9180049100-0-1	Failed
29.	MCULE-4018664519-0-1	Failed
30.	MCULE-3279207023-0-1	Passed
31.	MCULE-9774830352-0-1	Failed
32.	MCULE-8742796317-0-1	Failed
33.	MCULE-6766771092-0-11	Failed
34.	MCULE-7678621098-0-1	Passed
35.	MCULE-1175659191-0-1	Passed
36.	MCULE-3991253605-0-1	Passed
37.	MCULE-7026407753-0-3	Passed
38.	MCULE-3212232017-0-4	Failed
39.	MCULE-2848222492-0-1	Passed
40.	MCULE-9545019691-0-74	Passed
41.	MCULE-8894698072-0-2	Failed
42.	MCULE-1949229841-0-2	Passed
43.	MCULE-2364976076-0-11	Passed
44.	MCULE-2337612886-0-3	Failed
45.	MCULE-9983139545-0-2	Failed
46.	MCULE-2346913695-0-1	Passed
47.	MCULE-7595378623-0-1	Passed
48.	MCULE-1268978276-0-63	Passed
49.	MCULE-5436286666-0-1	Passed
50.	MCULE-9056345284-0-1	Failed
51.	MCULE-6613229794-0-1	Passed
52.	MCULE-1792852362-0-4	Failed

53.	MCULE-5543253227-0-1	Failed
54.	MCULE-6756956850-0-1	Passed
55.	MCULE-2959741432-0-3	Failed
56.	MCULE-1630554512-0-1	Passed
57.	MCULE-5429550474-0-1	Failed
58.	MCULE-9110513884-0-1	Passed
59.	MCULE-9920865629-0-8	Failed
60.	MCULE-1136944181-0-2	Failed
61.	MCULE-8757392030-0-1	Passed
62.	MCULE-7885124405-0-6	Failed
63.	MCULE-4333400439-0-3	Failed
64.	MCULE-5795139091-0-1	Passed
65.	MCULE-8922375714-0-2	Passed
66.	MCULE-6120922582-0-1	Passed
67.	MCULE-4694042030-0-4	Failed
68.	MCULE-7622376387-0-1	Passed
69.	MCULE-7882770900-0-1	Passed
70.	MCULE-8302247456-0-2	Passed
71.	MCULE-4470372384-0-1	Failed
72.	MCULE-3633342528-0-4	Passed
73.	MCULE-2771929429-0-3	Passed
74.	MCULE-4109133773-0-1	Passed
75.	MCULE-6625674793-0-1	Passed
76.	MCULE-6720977409-0-1	Passed
77.	MCULE-7929482340-0-1	Passed
78.	MCULE-1244449277-0-2	Passed
79.	MCULE-7551298769-0-1	Passed
80.	MCULE-7611227259-0-8	Failed
81.	MCULE-7563265724-0-1	Failed
82.	MCULE-4920383552-0-2	Passed
83.	MCULE-2230747440-0-20	Passed
84.	MCULE-7016970852-0-41	Passed
85.	MCULE-4134414820-0-3	Failed
86.	MCULE-6258460674-0-1	Passed
87.	MCULE-4031079253-0-1	Passed
88.	MCULE-5667035067-0-1	Passed
89.	MCULE-9508121818-0-6	Failed
90.	MCULE-6357350491-0-2	Passed
91.	MCULE-7695843923-0-2	Passed
92.	MCULE-7963939105-0-2	Passed
93.	MCULE-4834316893-0-2	Failed
94.	MCULE-5446518588-0-7	Failed
95.	MCULE-8700050471-0-4	Failed
96.	MCULE-6376548215-0-1	Failed
97.	MCULE-4281952551-0-2	Passed
98.	MCULE-5887067313-0-1	Passed
99.	MCULE-2357737612-0-5	Failed
100.	MCULE-9000936330-0-2	Passed

Examining hydrogen bond interactions, only two ligand hits, specifically MCULE-3872425295-0-7 and MCULE-8572723302-0-2, exhibited three and two hydrogen bonds, respectively, in contrast to the reference molecule, 5HA, which showed the presence of four conventional hydrogen bonds.

Throughout the binding interactions with the target protein BACE1, the reference drug, 5HA, displayed the presence of four conventional hydrogen bonds. The predicted ligands, particularly MCULE-3872425295-0-7 and MCULE-8572723302-0-2, exhibited lower ΔG values, indicating robust binding affinities with the target protein

Table 2. Binding energies and molecular interactions of ligand hits and the known inhibitor 5HA.

S. No.	Ligand hits	Binding energy	Types of molecular interactions
1.	MCULE-8572723302-0-2	-8.24	Van der Waals (Vdw), hydrogen bonds (HB), Pi-Anion, Pi-Donor hydrogen bond, Pi-Pi T-shaped, and Pi-Alkyl
2.	MCULE-3872425295-0-7	-8.83	Vdw, HBs, carbon-hydrogen bonds (CHB), Amide-pi Stacked, and Pi-Alkyl
3.	MCULE-9199128437-0-2	-8.19	Vdw, HBs, Pi-Anion, Alkyl and Pi-Alkyl
4.	MCULE-2491610851-0-1	-7.90	Vdw, HBs, halogen (fluorine), Amide-Pi Stacked, and Pi-Alkyl
5.	MCULE-4983453402-0-1	-7.84	Vdw, HBs, and Pi-Anion, Alkyl and Pi-Alkyl
6.	5HA (Control)	-7.82	Vdw, HBs, CHB, Pi-Donor hydrogen bond, Pi-Pi T-shaped, Amide-Pi Stacked, and Pi-Alkyl

residues.

Further analysis and selection of compounds were based on the presence of maximum hydrogen bonds and strong binding affinity compared with the control molecules. MCULE-3872425295-0-7, with a ΔG value of -8.83 kcal/mol, interacted with 17 residues through five distinct binding interactions, including Van der Waals, hydrogen bonds, carbon-hydrogen bonds, Amide-pi Stacked, and Pi-Alkyl interactions (Figure 2B). Similarly, MCULE-8572723302-0-2, displaying a ΔG value of -8.24 kcal/mol, interacted with 19 residues through six different binding interactions, namely Van der Waals, hydrogen bonds, Pi-Anion, Pi-Donor hydrogen bond, Pi-Pi T-shaped, and Pi-Alkyl interactions (Figure 3).

3.4 Evaluation of ligand potential for human intestinal absorption and blood-brain barrier permeation using Egan-Egg filtration

The Egan-Egg model, an essential component of ADME descriptors, has been employed to predict the viability of ligands for both passive human intestinal absorption (HIA) and permeation across the blood-brain barrier (BBB). The model delineates two distinct regions, yellow and white, which represent physicochemical spaces associated with significant BBB permeation and gastrointestinal (GI) absorption, respectively [50].

In the context of BBB penetration and HIA permeation, the Egan-Egg model categorizes ligands into yellow and white regions, designating their predictive positions for substantial BBB permeation and effective HIA permeation, respectively. Several ligand hits, including MCULE-3872425295-0-7, MCULE-8572723302-0-2, MCULE-2491610851-0-1, MCULE-4983453402-0-1, and MCULE-9199128437-0-2 displayed plausible HIA permeation. Notably, the first four ligand hits also demonstrated BBB permeation, which is a crucial characteristic in the design of neurodegenerative drug candidates. However, MCULE-9199128437-0-2 does not exhibit BBB permeability [51,52].

In addition, the reference drug, 5HA, displayed low HIA permeation but did not exhibit BBB permeation. Figure 4 illustrates the BOILED-Egg predictions for both ligands and reference molecules, where the blue and red dots represent the P-gp-positive and P-gp-negative molecules, respectively. This distinction highlights that ligands that are substrates of P-glycoprotein are expelled during BBB penetration, whereas non-substrate ligands have the potential to traverse the brain membrane.

3.5 Physicochemical characteristics analysis

The physicochemical properties of molecules, including Molecular Weight (MW), FCsp3 hybridization, Rotatable Bonds (RB), Hydrogen Bond Acceptor (HBA), Hydrogen Bond Donor (HBD), and Total Polar Surface Area (TPSA), play a critical role in the rapid prediction of the ADME attributes of investigational ligand molecules [53, 54]. The success of a compound is determined by its adherence to acceptable ranges of these physicochemical parameters.

SwissADME employs OpenBabel v.2.3.0 to calculate the ADME features and utilizes a fragment technique to estimate the Polar Surface Area (PSA). The BACE1 inhib-

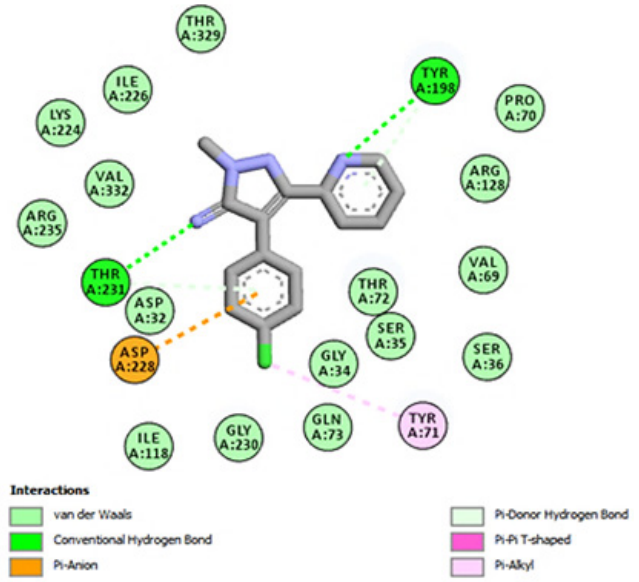

Fig. 3. 2D Illustration depicting the engagement between BACE1 and MCULE-8572723302-0-2 showing various molecular forces.

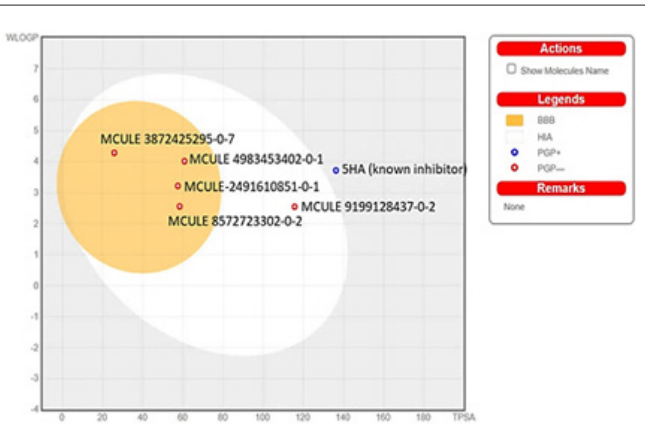

Fig. 4. Assessment of blood-brain barrier permeability and gut absorption for ligands and control molecules using the Egan-egg model.

Table 3. Physiochemical properties of ligands and known inhibitor 5HA.

Ligand	MW (g mol^{-1})	Fcsp^3	RB	HBA	HBD	MR	TPSA (Å^2)
5HA (known inhibitor)	578.72	0.35	15	6	4	160.08	136.22
MCULE-2491610851-0-1	314.31	0.62	3	7	1	78.78	58.35
MCULE-9199128437-0-2	310.39	0.31	3	4	2	77.79	115.65
MCULE-3872425295-0-7	289.16	0.07	2	2	0	78.8	25.78
MCULE-8572723302-0-2	284.74	0.07	2	2	2	80.25	57.46
MCULE-4983453402-0-1	240.68	0	1	2	1	59.83	60.77

Table 4. Lipophilicity of ligands and known inhibitor 5HA.

Ligand	iLOGP	XLOGP3	WLOGP	MLOGP
5HA (known inhibitor)	3.58	3.6	3.72	1.89
MCULE-2491610851-0-1	2.68	2.81	2.56	2.5
MCULE-9199128437-0-2	1.23	1.71	2.55	0.89
MCULE-3872425295-0-7	2.85	4.29	4.29	3.38
MCULE-8572723302-0-2	2.6	2.87	3.22	2.42
MCULE-4983453402-0-1	2.19	2.59	4.02	2.61

Table 5. Comparative solubility assessment of ligands and reference inhibitor 5HA.

Ligand	Log S (ESOL)	Log S (Ali)	Log S (SILICOS-IT)
5HA (known inhibitor)	-5.03	-6.15	-8.61
MCULE-2491610851-0-1	-3.66	-3.69	-3.3
MCULE-9199128437-0-2	-3.05	-3.75	-4.56
MCULE-3872425295-0-7	-4.83	-4.54	-7.12
MCULE-8572723302-0-2	-3.91	-3.74	-6.12
MCULE-4983453402-0-1	-3.49	-3.52	-5.18

itor, 5HA, serves as a reference with a Molecular Weight of 270.24 and FCsp3 of 0. Information regarding the compounds that successfully passed the toxicity assessment is shown in Table 3. These physicochemical insights contribute to the rapid assessment and prediction of ADME profiles of potential ligands.

3.6 Lipophilicity analysis of ligands and reference molecule 5HA

The evaluation of lipophilicity is of utmost importance in understanding the ability of a drug to dissolve in lipids or fats, as it offers insights into the potential interactions and absorption of the drug within lipid-rich environments, which subsequently affects its pharmacokinetic behavior in the body. The lipophilicity of a drug is typically measured using the partition coefficient (P), which is the ratio of the concentration of the drug in a nonpolar solvent (octanol) to its concentration in a polar solvent (water). A higher partition coefficient or lipophilicity indicates a greater likelihood of the drug being distributed and retained by lipid-rich tissues. Achieving optimal lipophilicity is crucial for the effectiveness of a drug, and balancing it is necessary to attain the appropriate pharmacokinetic properties for absorption, distribution, metabolism, and excretion within the body. During drug development, various computational and experimental methods have been used to assess and optimize lipophilicity [55, 56]. The analyzed compounds displayed a range of lipophilic characteristics, with iLOGP values ranging from 1.23 to 3.58, XLOGP values ranging from 1.71 to 4.29, WLOGP values ranging from 2.55 to 4.29, and MLOGP values ranging from 0.89 to 3.38 (Table 4). These values provide valuable information for understanding the lipophilic characteristics of ligands and their potential impact on pharmacokinetics.

3.7 Solubility analysis of ligands and reference molecule 5HA

The solubility of a drug is essential to understand its absorption, distribution, and effectiveness within the body. Drugs with poor solubility present difficulties in formulation and delivery. Solubility is determined by the maximum amount of substance that can dissolve in a solvent under specific conditions, such as temperature and pressure. SwissADME uses three methods for solubility studies: ESOL, Ali, and SILICOS-IT filters [57-61].

Based on the solubility analysis, the known inhibitor was classified as poorly to moderately soluble, falling within the optimum range. Conversely, some of the ligands exhibited moderate to good solubility. This information is crucial for understanding the potential challenges in drug formulation and delivery and for identifying ligands with desirable solubility profiles for further pharmaceutical development (Table 5).

3.8 Pharmacokinetic evaluation: Assessing safety and effectiveness

The evaluation of pharmacokinetics is of utmost importance in determining the safety and efficacy of a drug candidate. This process involves investigating the interaction of the compound with permeability glycoprotein (P-gp) and CYP enzymes and assessing whether it acts as a substrate or non-substrate. The skin permeability coefficient (Kp) is calculated using a regression model adapted from Potts and Guy [62, 63].

Table 6. Comparative pharmacokinetic parameters of ligands and reference inhibitor 5HA.

Ligands	CYP1A2 inhibitor	CYP2C19 inhibitor	CYP2C9 inhibitor	CYP2D6 inhibitor	CYP3A4 inhibitor
5HA (known inhibitor-BACE-1)	No	Yes	Yes	Yes	Yes
MCULE-2491610851-0-1	No	No	No	No	No
MCULE-9199128437-0-2	No	No	No	No	No
MCULE-3872425295-0-7	Yes	Yes	Yes	No	No
MCULE-8572723302-0-2	Yes	Yes	No	No	No
MCULE-4983453402-0-1	Yes	No	No	No	No

Table 7. Drug likeness of ligands and known inhibitor 5HA.

Ligand	Lipinski RO5	Ghose	Veber	Egan	Muegge
	violations				
5HA (known inhibitor)	1	3	1	1	0
MCULE-2491610851-0-1	0	0	0	0	0
MCULE-9199128437-0-2	0	0	0	0	0
MCULE-3872425295-0-7	0	0	0	0	0
MCULE-8572723302-0-2	0	0	0	0	0
MCULE-4983453402-0-1	0	0	0	0	0

Table 8. Comparative analysis of medicinal chemistry attributes in ligands & reference Iinhibitor 5HA.

Molecules	PAINS alerts	Brenk alerts	Lead-likeness violations	Synthetic Accessibility
5HA (known inhibitor)	0	0	3	4.79
MCULE-2491610851-0-1	0	0	0	3.72
MCULE-9199128437-0-2	0	0	0	3.43
MCULE-3872425295-0-7	0	1	1	2.85
MCULE-8572723302-0-2	0	0	0	2.81
MCULE-4983453402-0-1	0	1	1	2.18

A more negative Kp value indicates lower skin permeability for the molecule, indicating that the compound has a reduced permeation through the skin. Therefore, Kp negativity was associated with reduced skin permeability. This parameter is essential for evaluating the suitability of a drug candidate, particularly its ability to penetrate the skin barrier. The computed pharmacokinetic features of the ligand and control molecules are listed in Table 6.

3.9 Drug likeness assessment

Various sets of guidelines or filters, including Lipinski's Rule of Five, Ghose's Rule, Veber's Rule, Egan's Rule, and Muegge's Rule, are used in drug discovery and development to evaluate the drug-likeness of chemical compounds [64]. These rules are valuable tools for predicting the potential success of a compound as an orally active drug. Although there are slight variations in the considered physicochemical properties among the rules, such as molecular weight, LogP value, and the number of hydrogen bond donors and acceptors, they collectively contribute to the assessment of a compound's suitability.

Lipinski's Rule of Five (RO5) evaluates a compound based on four key properties: molecular weight, lipophilicity, hydrogen bond donors, and hydrogen bond acceptors [65, 66]. Veber's rule focuses on the oral bioavailability of a compound, specifically considering the number of rotatable bonds. Egan's rule assesses oral availability based on molecular weight, LogP, and hydrogen bond acceptors. Muegge's rule incorporates a range of properties, including molecular weight, lipophilicity, and the number of hydrogen bond donors and acceptors [67, 68] (Table 7). These rules collectively aid in gauging the drug-likeness of compounds and offer valuable insights into drug development.

3.10 Analysis of medicinal chemistry attributes

In the field of drug discovery, the term Pan-Assay Interference Compounds (PAINS) is used to describe chemical compounds that can interfere with the results of various biological assays, potentially leading to false-positive results in high-throughput screenings [69, 70]. These compounds often referred to as hits, exhibit nonspecific activity and can create unwanted interactions with assay components. PAINS compounds lack specificity for a particular target and demonstrate activity in a wide range of biological assays.

To address this issue, structural filters, called Brenk alerts or Brenk filters, have been developed. These filters were designed to identify problematic compounds in virtual or high-throughput screening campaigns for drug discovery. Similar to other medicinal chemistry filters, such as PAINS, Brenk alerts target-specific structural motifs identified through the analysis of compounds with undesirable assay interference properties.

During drug discovery, lead compounds, which are early-stage drug candidates with promising biological activity, are assessed for lead-likeness. This evaluation was based on criteria such as molecular weight, lipophilicity, hydrogen bond donors and acceptors, number of rotatable bonds, and topological polar surface area. It is important to note that these lead-likeness criteria are guidelines rather than strict rules and may vary based on the specific context and target class [68] (Table 8). These attributes contribute to the careful evaluation of compounds during drug dis-

covery and development.

3.11 Molecular dynamics simulation analysis

To evaluate the stability of the docked complexes, a Molecular Dynamics Simulation (MDS) was employed, and a graphical representation was generated illustrating the Root Mean Square Deviation (RMSD), Root Mean Square Fluctuation (RMSF), and Radius of Gyration. This analysis provides important insights into docked complexes' dynamic behavior and stability throughout the simulation.

3.12 RMSD, RMSF and Rg analysis

The Root Mean Square Deviation (RMSD) is a metric used to measure the square of the quadratic mean of the disparities between the anticipated and actual values within a sample, and it is commonly utilized to assess the stability of docked complexes. In this study, the RMSD values for the Cα atoms of BACE1-MCULE-8572723302-0-2, BACE1-MCULE-3872425295-0-7, and BACE1-5HA complexes were determined to be approximately 5 ns. The RMSD values for the BACE1-MCULE-8572723302-0-2 and BACE1-MCULE-3872425295-0-7 complexes were 1.32 nm and 1.36 nm, respectively. The RMSD value for the reference molecule BACE1-5HA was 1.46 nm.

The RMSD plot in Figure 5A illustrates the dynamic behavior and stability of the docked complexes over time. Notably, the complex formed by BACE1-MCULE-3872425295-0-7 displayed superior stability compared to the complex formed by the reference molecule. This analysis provides crucial insights into the structural fluctuations and overall stability of the docked complexes during Molecular Dynamics simulations, offering valuable information for the evaluation of potential drug candidates.

RMSF is a useful tool for evaluating the flexibility of docked complexes and is often employed to quantify variations by comparing initial and final fluctuations. Average RMSF values for the docked complexes BACE1-MCULE-8572723302-0-2 (1.4 nm), BACE1-MCULE-3872425295-0-7 (1.84 nm), and BACE1-5HA (control) (1.87 nm). This analysis provides valuable insights into the structural fluctuations of docked complexes during molecular dynamics simulations (Figure 5B).

The decreasing trend of the radii of gyration (Rg) with increasing compactness of the docked complexes is noteworthy. The average Rg values for BACE1-MCULE-3872425295-0-7, BACE1-MCULE-8572723302-0-2, and BACE1-MCULE-5HA (control) are 3.11 nm, 3.14 nm, and 3.27 nm, respectively (Figure 5C). This analysis provides crucial information about the structural characteristics and compactness of docked complexes during molecular dynamics simulations, which can be useful in further investigations.

This study employed a comprehensive screening process using Pfizer's Lipinski's Rule of Five criteria to identify potential drug candidates targeting Alzheimer's Disease, specifically focusing on BACE1. From an initial pool of over two million candidates, 100 promising ligands have emerged. Further evaluation based on the binding free energy and hydrogen bond formation narrowed down the selection to five standout molecules. These results played a crucial role in refinement, leading to the identification of two lead ligands with binding affinities comparable to those of the control drug, 5HA. Docking simulations and toxicity assessments provided valuable insights into the interactions between these ligands and the BACE1 binding pocket. The structural interactions, illustrated in Figures 4 and 6, highlight the bonding modes and residues engaged by MCULE-3872425295-0-7 and MCULE 8572723302-0-2, laying the groundwork for linking these interactions with potential drug candidates.

According to the BOILED-Egg filtration model, the control drug exhibited limited permeation through HIA or BBB barriers. In contrast, MCULE 8572723302-0-2 successfully penetrated the BBB and HIA barriers, whereas MCULE-3872425295-0-7 -2 only penetrated the HIA barrier. Assessments of medicinal chemistry attributes indicated promising features without alerts or violations. However, the synthetic accessibility of these compounds was lower than that of the control. Additional stability as-

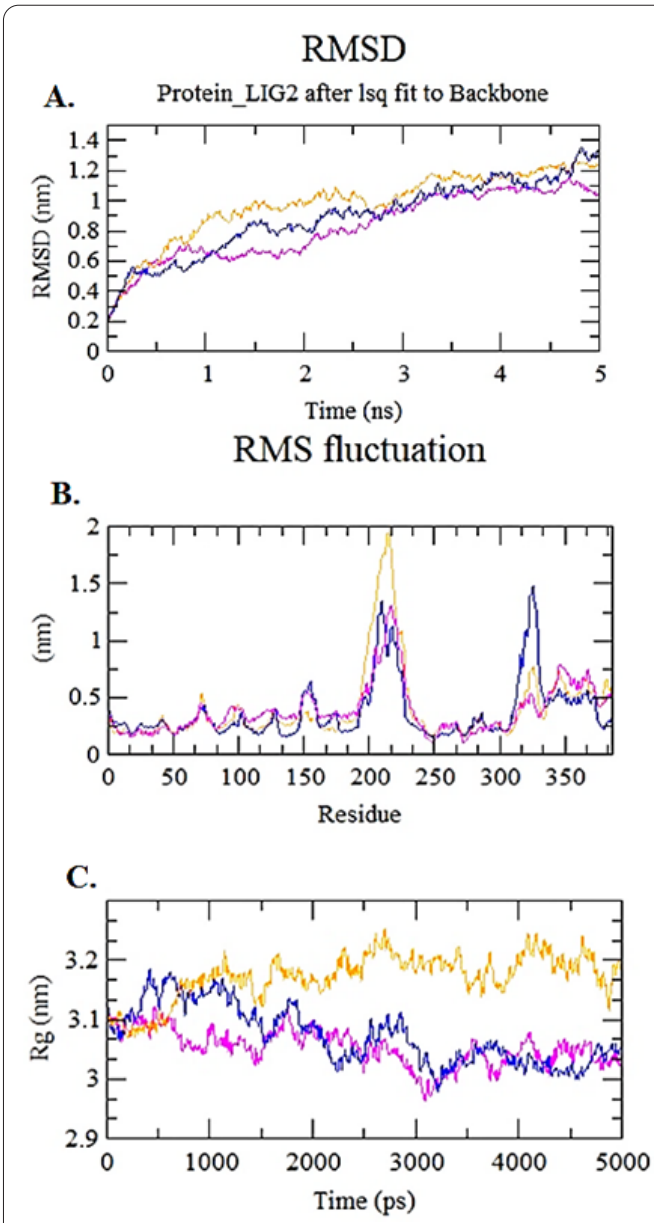

Fig. 5. **(A)** RMSD plot depicting structural stability during Molecular Dynamics Simulation for BACE1 complexes with MCULE-3872425295-0-7 (magenta), MCULE-8572723302-0-2 (blue), and 5HA (control) (orange). **(B)** RMSF plot illustrating structural fluctuations for the same complexes. **(C)** Rg plot showing overall structural characteristics. Distinct colors represent different ligands, facilitating comparative dynamic analysis.

sessments through Molecular Dynamics (MD) simulations provided crucial insights into the complexes formed by the top two ligand hits and the reference drug, 5HA. The lead ligand MCULE 8572723302-0-2 exhibited exceptional stability in the docking complex with BACE1, suggesting a more robust interaction than the reference molecule. These collective findings underscore the potential of lead ligands, especially MCULE 8572723302-0-2 and MCULE-3872425295-0-7, as promising drug candidates for addressing treatment. Their strong binding affinities, favorable characteristics for oral absorption, and stability in interactions with the target protein position them as compelling candidates for further development and optimization in the pursuit of potential drugs for Alzheimer 's disease treatment.

4. Conclusion

Alzheimer's has a considerable impact on the physiological well-being and self-care capabilities of the elderly, and it remains a critical global healthcare challenge. Research on the pathophysiological and neuropathological aspects of AD is ongoing and meticulous. Current AD treatments aim to rectify the neurotransmitter imbalance. Comprehensive care for individuals with AD requires the management of vascular risk factors, such as hyperlipidemia, diabetes, and hypertension. Holistic patient care involves monitoring of hydration, sleep patterns, and nutritional status. Clinical trial setbacks for AD disease-modifying therapies result from factors such as delayed intervention, suboptimal dosages, misdirected primary treatment targets, and incomplete understanding of AD's pathophysiology of AD. An enhanced understanding of AD's multifaceted pathophysiology of AD is essential for refining therapeutic strategies and advancing effective interventions. Based on a comprehensive analysis of various ligands, MCULE-3872425295-0-7 emerged as the most promising drug candidate. This conclusion is based on a thorough assessment of factors such as binding affinity, pharmacokinetics, and potential therapeutic effects. MCULE-3872425295-0-7 displays superior attributes in these aspects compared to other ligands, indicating its potential as a highly effective drug candidate. This conclusion was supported by a holistic evaluation of the data, which suggested that MCULE-3872425295-0-7 stood out among the candidates studied.

Acknowledgments

This research work was funded by Institutional Fund Projects under grant no. (IFPIP:64-828-1443). The authors gratefully acknowledge the technical and financial support provided by the Ministry of Education and King Abdulaziz University, DSR, Jeddah, Saudi Arabia.

Consent for publications

The author read & approved the final manuscript for publication.

Ethics approval and consent to participate

There is no use of human or animals in the present research.

Conflict of interest

The authors declare that they have nothing to disclose.

Informed consent

The authors declare not used any patients in this research.

Author's contribution

HASM: Helps to write the manuscript draft and design the concept. MSM: Helped to second draft manuscript and analysis, AA: contributed to docking work. SA: Docking analysis and table work. AA: Edit manuscript, MIA: Helped to design the docking work. RAA: simulation study. AHH: Drug Likeness Assessment. ZMS: contributed to the analysis, and editing manuscript.MR: helped to edit the manuscript and hypothesis.

References

1. Hebert LE, Weuve J, Scherr PA, Evans DA (2013) Alzheimer disease in the United States (2010-2050) estimated using the 2010 census. Neurology 80(19): doi: 10.1212/WNL.0b013e31828726f5
2. Association A (2018) 2018 Alzheimer's Disease Facts and Figures. Alzheimers dement 14(3): 367-429. https://doi.org/10.1016/j.jalz.2018.02.001
3. Troutwine BR, Hamid L, Lysaker CR, Strope TA, Wilkins HM (2022) Apolipoprotein E and Alzheimer's disease. Acta Pharm Sin B 12(2):496-510. doi: 10.1016/j.apsb.2021.10.002.
4. Tang MX, Stern Y, Marder K, Bell K, Gurland B, Lantigua R, Andrews H, Feng L, Tycko B, Mayeux R (1998) The APOE-ε4 allele and the risk of Alzheimer disease among African Americans, whites, and Hispanics. JAMA 279(10): doi: 10.1001/jama.279.10.751.
5. Marca-Ysabel MV, Rajabli F, Cornejo-Olivas M, Whitehead PG, Hofmann NK, Illanes Manrique MZ, Otani DMV, Neyra AKM, Suarez SC, Vega MM, Adams LD, Mena PR, Rosario I , Cuccaro ML, Vance JM, Beecham GW, Custodio N, Montesinos R, Mazzetti Soler PE, Pericak-Vance MA (2021) Dissecting the role of Amerindian genetic ancestry and the ApoE ε4 allele on Alzheimer disease in an admixed Peruvian population. Neurobiol Aging 101:298.e11-298.e15. doi: 10.1016/j.neurobiolaging.2020.10.003
6. Pasqualetti G, Thayanandan T, Edison P (2022) Influence of genetic and cardiometabolic risk factors in Alzheimer's disease. Ageing Res Rev 81:101723.doi: 10.1016/j.arr.2022.101723.
7. Silva MVF, Loures CDMG, Alves LCV, De Souza LC, Borges KBG, Carvalho MDG (2019) Alzheimer's disease: Risk factors and potentially protective measures. J Biomed Sci 26(1): 33.doi: 10.1186/s12929-019-0524-y.
8. James BD, Bennett DA (2019) Causes and Patterns of Dementia: An Update in the Era of Redefining Alzheimer's Disease. Annu Rev Public Health 1:40:65-84. doi: 10.1146/annurev-publhealth-040218-043758
9. Ren Y, Savadlou A, Park S, Siska P, Epp JR, Sargin D (2023) The impact of loneliness and social isolation on the development of cognitive decline and Alzheimer's Disease. Front Neuroendocrinol 69:101061. doi: 10.1016/j.yfrne.2023.101061
10. Zhuo JM, Wang H, Praticò D (2011) Is hyperhomocysteinemia an Alzheimer's disease (AD) risk factor, an AD marker, or neither? Trends Pharmacol Sci 32(9):562-71. doi: 10.1016/j.tips.2011.05.003.
11. Wang D, Chen F, Han Z, Yin Z, Ge X, Lei P (2021) Relationship Between Amyloid-β Deposition and Blood–Brain Barrier Dysfunction in Alzheimer's Disease. Front Cell Neurosci 19:15:695479. doi: 10.3389/fncel.2021.695479.
12. Kim K, Wang X, Ragonnaud E, Bodogai M, Illouz T, DeLuca, McDevitt RA, Gusev F, Okun E, Rogaev E, Biragyn A (2021) Therapeutic B-cell depletion reverses progression of Alzheimer's disease. Nat Commun 12;12(1):2185. doi: 10.1038/s41467-021-

22479-4.
13. Zhang Y, Liu T, Lanfranchi V, Yang P (2023) Explainable Tensor Multi-Task Ensemble Learning Based on Brain Structure Variation for Alzheimer's Disease Dynamic Prediction. IEEE J Transl Eng Health Med 11:1-12. doi: 10.1109/JTEHM.2022.3219775.
14. Kumar S, Oh I, Schindler S, Lai AM, Payne PRO, Gupta A (2021) Machine learning for modeling the progression of Alzheimer disease dementia using clinical data: A systematic literature review. JAMIA Open 4(3):ooab052. doi: 10.1093/jamiaopen/ooab052.
15. Kim Y, Kim J, Son M, Lee J, Yeo I, Choi KY, Kim H, Kim BC, Lee KH, Kim Y (2022) Plasma protein biomarker model for screening Alzheimer disease using multiple reaction monitoring-mass spectrometry. Sci Rep Sci Rep 12(1):1282.doi: 10.1038/s41598-022-05384-8.
16. Green C, Shearer J, Ritchie CW, Zajicek JP (2011) Model-based economic evaluation in Alzheimer's disease: A review of the methods available to model Alzheimer's disease progression. Value Health 14(5):621-30.doi: 10.1016/j.jval.2010.12.008.
17. Calabrò M, Rinaldi C, Santoro G, Crisafulli C (2020) The biological pathways of Alzheimer disease: a review. AIMS Neurosci 8(1):86-132.doi: 10.3934/Neuroscience.2021005.
18. Lee HN, Jeong MS, Jang SB (2021) Molecular characteristics of amyloid precursor protein (App) and its effects in cancer. Int J Mol Sci 22(9):4999. doi: 10.3390/ijms22094999.
19. Delvaux E, Bentley K, Stubbs V, Sabbagh M, Coleman PD (2013) Differential processing of amyloid precursor protein in brain and in peripheral blood leukocytes. Neurobiol Aging 34(6):1680-6. doi: 10.1016/j.neurobiolaging.2012.12.004.
20. Sayad A, Najafi S, Hussen BM, Abdullah ST, Movahedpour A, Taheri M, Hajiesmaeili M (2022) The Emerging Roles of the β-Secretase BACE1 and the Long Non-coding RNA BACE1-AS in Human Diseases: A Focus on Neurodegenerative Diseases and Cancer. Front Aging Neurosci 14:853180. doi: 10.3389/fnagi.2022.853180.
21. Hampel H, Vassar R, De Strooper B, Hardy J, Willem M, Singh N, Zhou J, Yan R, Vanmechelen E, Vos AD, Nisticò R, Corbo M, Imbimbo BP, Streffer J, Voytyuk I, Timmers M, Monfared ABT, Irizarry M, Albala B, Koyama A, Watanabe N, Kimura T, Yarenis L, Lista S, Kramer L, Vergallo A (2021) The β-Secretase BACE1 in Alzheimer's Disease. Biol Psychiatry 89(8):745-756. doi: 10.1016/j.biopsych.2020.02.001.
22. Taylor HA, Przemylska L, Clavane EM, Meakin PJ (2022) BACE1: More than just a β-secretase. Obes Rev 23(7):e13430. doi: 10.1111/obr.13430.
23. Wang Z, Xu Q, Cai F, Liu X, Wu Y, Song W (2019) BACE2, a conditional β-secretase, contributes to Alzheimer's disease pathogenesis. JCI Insight 4(1):e123431. doi: 10.1172/jci.insight.123431.
24. Aow J, Huang TR, Thinakaran G, Koo EH (2022) Enhanced cleavage of APP by co-expressed Bace1 alters the distribution of APP and its fragments in neuronal and non-neuronal cells. Mol Neurobiol 59(5):3073-3090. doi: 10.1007/s12035-022-02733-6.
25. Bazzari FH, Bazzari AH. (2022) BACE1 Inhibitors for Alzheimer's Disease: The Past, Present and Any Future? Molecules 27(24):8823. doi: 10.3390/molecules27248823.
26. Liu L, Lauro BM, Ding L, Rovere M, Wolfe MS, Selkoe DJ (2019) Multiple BACE1 inhibitors abnormally increase the BACE1 protein level in neurons by prolonging its half-life. Alzheimers Dement 15(9):1183-1194. doi: 10.1016/j.jalz.2019.06.3918.
27. Vassar R. (2014) BACE1 inhibitor drugs in clinical trials for Alzheimer's disease. Alzheimers Res Ther 24;6(9):89. doi: 10.1186/s13195-014-0089-7.
28. Choi YA, Song IS, Choi MK (2018) Pharmacokinetic drug-drug interaction and responsible mechanism between memantine and cimetidine. Pharmaceutics 10(3):119. doi: 10.3390/pharmaceutics10030119.
29. Sharma K (2019) Cholinesterase inhibitors as Alzheimer's therapeutics (Review). Mol Med Rep 20(2):1479-1487. doi: 10.3892/mmr.2019.10374.
30. Khan I, Akhtar S, Ahmad Khan MK (2021) Lifestyle-based health awareness using digital gadgets and online interactive platforms. NeuroPharmac Journal 12: 295-310. doi: 10.37881/1.638
31. Long JM, Holtzman DM (2019) Alzheimer Disease: An Update on Pathobiology and Treatment Strategies. Cell 179(2):312-339. doi: 10.1016/j.cell.2019.09.001.
32. Yiannopoulou KG, Papageorgiou SG (2020) Current and Future Treatments in Alzheimer Disease: An Update. J Cent Nerv Syst Dis 12:1179573520907397. doi: 10.1177/1179573520907397
33. Burley SK, Bhikadiya C, Bi C, Bittrich S, Chen L, Crichlow G V. Burley SK, Bhikadiya C, Bi C, Bittrich S, Chen L, Crichlow GV, Duarte JM, Dutta S, Fayazi M, Feng Z, Flatt JW, Ganesan SJ, Goodsell DS, Ghosh S, Green RK, Guranovic V, Henry J, Hudson BP, Lawson CL, Liang Y, Lowe R, Peisach E, Persikova I, Piehl DW, Rose Y, Sali A, Segura J, Sekharan M , Shao C, Vallat B, Voigt M, Westbrook JD, Whetstone S, Young JY, Zardecki C (2022) RCSB Protein Data Bank: Celebrating 50 years of the PDB with new tools for understanding and visualizing biological macromolecules in 3D. Protein Sci 31(1):187-208. doi: 10.1002/pro.4213.
34. Bank PD. RCSB PDB: Homepage. Rcsb Pdb. 2019.
35. Brooks BR, Brooks CL, Mackerell AD, Nilsson L, Petrella RJ, Roux B, Won Y, Archontis G, Bartels C, Boresch S, Caflisch A, Caves L, Cui Q, Dinner A R, Feig M, Fischer S, Gao J, Hodoscek M, Im W, Kuczera K, Lazaridis T, Ma J, Ovchinnikov V, Paci E, Pastor R W, Post C B, Pu J Z, Schaefer M, Tidor B, Venable R M, Woodcock H L, Wu X, Yang W, York D M, Karplus M (2009) CHARMM: The biomolecular simulation program. J Comput Chem. J Comput Chem 30(10):1545-614. doi: 10.1002/jcc.21287.
36. Cheng T, Li Q, Zhou Z, Wang Y, Bryant SH (2012) Structure-based virtual screening for drug discovery: A problem-centric review. AAPS J 14(1):133-41. doi: 10.1208/s12248-012-9322-0.
37. Maia EHB, Assis LC, de Oliveira TA, da Silva AM, Taranto AG (2020) Structure-Based Virtual Screening: From Classical to Artificial Intelligence. Front Chem 8:343. doi: 10.3389/fchem.2020.00343.
38. O'Boyle NM, Morley C, Hutchison GR (2008) Pybel: A Python wrapper for the OpenBabel cheminformatics toolkit. Chem Cent J 2:5. doi: 10.1186/1752-153X-2-5.
39. Sharma S, Kumar P, Chandra R. (2019) Applications of BIOVIA materials studio, LAMMPS, and GROMACS in various fields of science and engineering. Book: Molecular Dynamics Simulation of Nanocomposites using BIOVIA Materials Studio, Lammps and Gromacs. doi: 10.1016/B978-0-12-816954-4.00007-3.
40. Biovia. Biovia Discovery Studio® (2020) Comprehensive Modeling and Simulations for Life Sciences Datasheet. Dassault Systemes: The 3D Experience Company.
41. Rizvi SMD, Shakil S, Haneef M (2013) A simple click by click protocol to perform docking: Autodock 4.2 made easy for non-bioinformaticians. EXCLI J 12:831-57.
42. Morris GM, Goodsell DS, Huey R, Olson AJ (1996) Distributed automated docking of flexible ligands to proteins: Parallel applications of AutoDock 2.4. J Comput Aided Mol Des 10(4):293-304. doi: 10.1007/BF00124499.
43. Eberhardt J, Santos-Martins D, Tillack AF, Forli S (2021) AutoDock Vina 1.2.0: New Docking Methods, Expanded Force Field, and Python Bindings. J Chem Inf Model 61(8):3891-3898. doi: 10.1021/acs.jcim.1c00203.

44. Butt SS, Badshah Y, Shabbir M, Rafiq M (2021) Molecular Docking Using Chimera and Autodock Vina Software for Nonbioinformaticians. JMIR Bioinform Biotech 1(1). doi: 10.2196/14232.
45. Bakchi B, Krishna AD, Sreecharan E, Ganesh VBJ, Niharika M, Maharshi S, Bulti B, Krishna, Dileep A, Sreecharan, Ekambarapu Ganesh, Jaya VB, Niharika, Muraboina, Suryadevara M, Puttagunta, Babu S , Sigalapalli, Kumar D, Bhandare, Richie R, Shaik, Afzal B (2022) An overview on applications of SwissADME web tool in the design and development of anticancer, antitubercular and antimicrobial agents: A medicinal chemist's perspective. J Mol Struct 1259, article id. 132712. doi: 10.1016/j.molstruc.2022.132712.
46. Deb S, Reeves AA, Hopefl R, Bejusca R. (2021) Adme and pharmacokinetic properties of remdesivir: Its drug interaction potential. Pharmaceuticals 14(7):655.doi: 10.3390/ph14070655.
47. Shou WZ (2020) Current status and future directions of high-throughput ADME screening in drug discovery. J Pharm Anal 10(3):201-208. doi: 10.1016/j.jpha.2020.05.004.
48. Ahmad Khan MK, Akhtar S, Al-Khodairy F (2021) Molecular docking approach to elucidate metabolic detoxification pathway of polycyclic aromatic hydrocarbons. NeuroPharmac Journal 6 (1): 150-161. doi: 10.37881/1.613.
49. Khan I, Khan MKA, Akhtar S (2023) Evaluation of Terpenoids as Dipeptidyl Peptidase 4 Lead Molecules: Molecular Docking and Dynamics Simulation Study. Biointerface Res Appl Chem. 13(4). https://doi.org/10.33263/BRIAC134.376.
50. Daina A, Zoete V (2016) A BOILED-Egg To Predict Gastrointestinal Absorption and Brain Penetration of Small Molecules. ChemMedChem ChemMedChem 6;11(11):1117-21. doi: 10.1002/cmdc.201600182.
51. Hasan MM, Khan Z, Chowdhury MS, Khan MA, Moni MA, Rahman MH (2022) In silico molecular docking and ADME/T analysis of Quercetin compound with its evaluation of broad-spectrum therapeutic potential against particular diseases. Inform Med Unlocked 29:100894. https://doi.org/10.1016/j.imu.2022.100894.
52. Parameswari P, Devika R (2019) In silico molecular docking studies of quercetin compound against anti-inflammatory and anticancer proteins. Res J Pharm Technol 12(11):5305-5309. doi: 10.5958/0974-360X.2019.00919.3.
53. Prasanna S, Doerksen R (2009) Topological Polar Surface Area: A Useful Descriptor in 2D-QSAR. Curr Med Chem 16(1):21-41. doi: 10.2174/092986709787002817.
54. Sun M, Ma P, Chen C, Pang Z, Huang Y, Liu X, Wang P (2023) Physiochemical characteristics, morphology, and lubricating properties of size-specific whey protein particles by acid or ion aggregation. Int J Biol Macromol 252:126346.doi: 10.1016/j.ijbiomac.2023.126346.
55. Waring MJ (2010) Lipophilicity in drug discovery. Expert Opin Drug Discov 5(3):235-48. doi: 10.1517/17460441003605098.
56. Arnott JA, Planey SL (2012) The influence of lipophilicity in drug discovery and design. Vol. 7, Expert Opinion on Drug Discovery. Expert Opin Drug Discov 7(10):863-75. doi: 10.1517/17460441.2012.714363.
57. Lipinski CA, Lombardo F, Dominy BW, Feeney PJ (2001) Experimental and computational approaches to estimate solubility and permeability in drug discovery and development settings. Adv Drug Deliv Rev 46(1-3):3-26. doi: 10.1016/s0169-409x(00)00129-0.
58. Savjani KT, Gajjar AK, Savjani JK (2012) Drug Solubility: Importance and Enhancement Techniques. ISRN Pharm 2012:195727. doi: 10.5402/2012/195727.
59. Ali J, Camilleri P, Brown MB, Hutt AJ, Kirton SB (2012) Revisiting the general solubility equation: In silico prediction of aqueous solubility incorporating the effect of topographical polar surface area. J Chem Inf Model 52(2):420-8. doi: 10.1021/ci200387c.
60. Delaney JS (2004) ESOL: Estimating aqueous solubility directly from molecular structure. J Chem Inf Comput Sci 44(3):1000-5. doi: 10.1021/ci034243x.
61. Chen J, Zheng S, Zhao H, Yang Y (2021) Structure-aware protein solubility prediction from sequence through graph convolutional network and predicted contact map. J Cheminform 13(1):7. doi: 10.1186/s13321-021-00488-1.
62. O'Hara K (2016) Paediatric pharmacokinetics and drug doses. Aust Prescr 39(6):208-210. doi: 10.18773/austprescr.2016.071.
63. Peng Y, Cheng Z, Xie F (2021) Evaluation of pharmacokinetic drug-drug interactions: A review of the mechanisms, in vitro and in silico approaches. Metabolites 11(2):75. doi: 10.3390/metabo11020075.
64. Muegge I, Heald SL, Brittelli D (2001) Simple selection criteria for drug-like chemical matter. J Med Chem 44(12):1841-6. doi: 10.1021/jm015507e.
65. Karami TK, Hailu S, Feng S, Graham R, Gukasyan HJ (2022) Eyes on Lipinski's Rule of Five: A New "Rule of Thumb" for Physicochemical Design Space of Ophthalmic Drugs. J Ocul Pharmacol Ther 38(1):43-55. doi: 10.1089/jop.2021.0069.
66. Mullard A (2018) Re-assessing the rule of 5, two decades on. Nat Rev Drug Discov 17(11):777. doi: 10.1038/nrd.2018.197.
67. Yalçın S, Yalçınkaya S, Ercan F (2021) Determination of Potential Drug Candidate Molecules of the Hypericum perforatum for COVID-19 Treatment. Curr Pharmacol Rep 7(2):42-48. doi: 10.1007/s40495-021-00254-9.
68. Bickerton GR, Paolini G V., Besnard J, Muresan S, Hopkins AL (2012) Quantifying the chemical beauty of drugs. Nat Chem 4(2):90-8.doi: 10.1038/nchem.1243.
69. Mahmud S, Paul GK, Biswas S, Kazi T, Mahbub S, Mita MA, Afrose S, Islam A, Ahaduzzaman S, Hasan R, Shimu SS, Promi MM, Shehab MN, Rahman E, Sujon KM , Alom W, Modak A, Zaman S, Uddin S, Emran TB, Islam S, Saleh A (2022) phytochemdb: a platform for virtual screening and computer-aided drug designing. Database (Oxford) 2022(2022):baac002. doi: 10.1093/database/baac002.
70. Dominguez Huarcaya LR, Dominguez Ríos MF, Mohammadi MR, Rahimi Z (2023) The role of microglia in depression. Cell Mol Biomed Rep 4(2):74-87. doi: 10.55705/cmbr.2023.409233.1162.